energy&fuels

Article

Effects of substitution on counterflow ignition and extinction of C3 and C4 alcohols

Adamu Alfazazi, Ulrich Niemann, Hatem M Selim, Robert J. Cattolica, and S. Mani Sarathy

Energy Fuels, **Just Accepted Manuscript** • DOI: 10.1021/acs.energyfuels.6b00518 • Publication Date (Web): 17 Jun 2016

ACS Publications

Energy & Fuels is published by the American Chemical Society. 1155 Sixteenth Street N.W., Washington, DC 20036

Effects of substitution on counterflow ignition and extinction of C3 and C4 alcohols

Adamu Alfazazi,[a] Ulrich Niemann,[b] Hatem Selim,[a] Robert J. Cattolica,[b] Mani S. Sarathy,*[a]*

[a]King Abdullah University of Science and Technology (KAUST), Clean Combustion Research Center (CCRC), Thuwal 23955-6900, Saudi Arabia.

[b]Department of Mechanical and Aerospace Engineering, University of California, San Diego, La Jolla, CA 92093-0411, USA.

KEYWORDS. Alcohol fuels; Extinction limits; Autoignition temperatures; Counterflow diffusion flames; Radical index

ABSTRACT. Dwindling reserves and inherent uncertainty in the price of conventional fuels necessitates a search for alternative fuels. Alcohols represent a potential source of energy for the future. The structural features of an alcohol fuel have a direct impact on combustion properties. In particular, substitution in alcohols can alter the global combustion reactivity. In this study, experiments and numerical simulations were conducted to investigate the critical conditions of extinction and autoignition of *n*-propanol, *1*-butanol, *iso*-propanol and *iso*-butanol in non-premixed diffusion flames. Experiments were carried out in the counterflow configuration, while simulations were conducted using a skeletal chemical kinetic model for the C3 and C4 alcohols. The fuel stream consists of the pre-vaporized fuel diluted with nitrogen, while the oxidizer

stream is air. The experimental results show that autoignition temperatures of the tested alcohols increase in the following order: *iso*-propanol > *iso*-butanol > *1*-butanol ≈ *n*-propanol. The simulated results for the branched alcohols agree with the experiments, while the autoignition temperature of *1*-butanol is slightly higher than that of *n*-propanol. For extinction, the experiments show that the extinction limits of the tested fuels increase in the following order: *n*-propanol ≈ *1*-butanol > *iso*-butanol > *iso*-propanol. The model suggests that the extinction limits of *1*-butanol is slightly higher than *n*-propanol with extinction strain rate of *iso*-butanol and *iso*-propanol maintaining the experimentally observed trend. The transport weighted enthalpy (TWE) and radical index (Ri) concepts were utilized to rationalize the observed reactivity trends for these fuels.

1. Introduction

As a result of an increase in the use of cars, harmful emissions of soot and NOx have become a serious global issue. To circumvent the issues related to pollution and carbon emissions, there is a need to explore the use of alternative fuels, such as alcohols.[1] Alcohols are oxygen-rich fuels, and when derived from biomass they are considered as carbon neutral.[2] Also, C1-C4 alcohols have high octane rating and low ignition propensity.[1] Therefore, when used as additives, alcohols are found to increase the performance of the spark ignition (SI) engines and reduce CO and particulate matter emissions. Previous studies by Agarwal et al.,[3] show that a blend of ethanol or *1*-butanol with a gasoline can reduce knocking tendency in the SI engine while a blend of diesel fuel with some percentage of these alcohols can reduce CO and NOx emission.

Moss et al.[4] investigated the high temperature reactivity of four butanol isomers in a shock tube, and found that *1*-butanol is the most reactive while *tert*-butanol is the least reactive. Veloo et al.[5] carried out a flame propagation study of all four butanol isomers using the counterflow

premixed twin-flame technique. They observed a similar reactivity for *1*-butanol, *iso*-butanol and *sec*-butanol. A comparative study on ignition delay times of alcohols by Noorani et al.[6] concluded that the high temperature ignition delay time of all normal alcohols (with the exception of methanol) is similar for a given stoichiometry. In separate studies, Beeckmann et al.[7] and Sarathy et al.,[1] noted a similarity in the burning velocities of *n*-propanol, *1*-butanol and ethanol at equivalence ratios between 0.8 and 1.1. A similar observation was made by Veloo et al.,[8] when measuring laminar flame speeds of methanol, ethanol and *1*-butanol at a range of equivalence ratios.

Many studies have reported the combustion properties of these important alcohols. However, studies about their autoignition and extinction behavior in counterflow diffusion flames remain scarce, as reviewed in detail by Sarathy et al.,[1] albeit they are important for validating high temperature ignition and flame chemistry in kinetic models. Counterflow diffusion flame studies are more representative of combustion modes in practical non-premixed combustors, while also enabling validation of both transport and kinetics in reacting flows.

As far as authors can tell, there is no study on ignition temperatures of *n*-propanol and *iso*-propanol in the counterflow diffusion flame. The only extinction data of *n*-propanol and *iso*-propanol in counterflow diffusion flame was given by Veloo et.al.[9] They carried out their experiment using oxygen as the oxidizer and they noted a lower reactivity for *iso*-propanol as compared to *n*-propanol. Through sensitivity analysis, they found that the difference in reactivity of *n*-propanol and *iso*-propanol is mainly because the former produces higher concentrations of formaldehyde that forms formyl radicals whose subsequent reactions promote reactivity. Their numerical simulation was carried out using two models; Curran et al.[10] model and a combination

of USC model II[11] and Curran et al's model. Overall, the combined mechanism showed a better agreement with the experiment than Curran et al's model.

Similarly, the only *1*-butanol and *iso*-butanol ignition data in the counterflow diffusion flame came from Brady et al.[12] Extinction data for *1*-butanol was previously provided by Veloo et al.,[8] and Hashimoto et al.,[13] while for the three butanol isomers was given by D. Kyritsis et al.[14] Brady et al.[12] employed a high pressure counterflow burner to study the effects of molecular structure on ignition temperatures of four butanol isomers at fuel mole fraction, $X_f = 0.15$ and pressure-weighted strain rate range of (200-400) 1/s. They noted higher ignition temperatures for *iso*-butanol as compared to *1*-butanol. They simulated their result using butanol models by Sarathy et al.[15] and Merchant et al.[16] Overall, both models predicted the trends observed in the experiment, but slightly over predicted the ignition temperatures. Kyritsis et al.[14] compared the extinction limits of three butanol isomers at different equivalence ratios and explained the observed reactivity of the fuels in terms of their bond dissociation energies. They noted a higher extinction limits for *1*-butanol as compared to *iso*-butanol mainly because *1*-butanol has more inner carbon atoms with smaller bond dissociation energies. So, few extinction studies of these fuels have been carried out but not autoignition studies.

Comparison of ignition and extinction data on these important classes of fuels in the counterflow still remain scarce over wide range of strain rate. For this reason, an experimental and kinetic modelling study is carried out on *1*-butanol (nc4h9oh), *iso*-butanol (ic4h9oh), *n*-propanol (nc3h7oh) and *iso*-propanol (ic3h7oh) fuels in the counterflow flame configuration at fuel mole fraction, $X_f = 0.4$ and various strain rates. This study aims at providing additional experimental data and numerical simulations for further insight into the ignition/extinction behavior of C3 and C4 alcohols in a non-uniform flow field. These properties were selected

because they are sensitive to both chemical kinetics and transport, and hence could be used to validate chemical kinetic models. Another goal is to provide an understanding on the effects of substitution (e.g., CH_3 and OH) on alcohol fuel reactivity in flames, as previously done for hydrocarbon fuels.[17,18] To this end, the critical conditions of autoignition and extinction of *1*-butanol, *n*-propanol, *iso*-butanol and *iso*-propanol were studied in the counterflow configuration.

2. Description of Experimental and Numerical procedures

2.1. Experimental Procedure

The experimental measurements were carried out using the counterflow diffusion flame facility at University of California San Diego. Figure 1 shows a schematic diagram of the counterflow configuration. A more detailed explanation of the facility has been given previously.[19,20] In summary, the burner consists of two-opposing ducts. Preheated air is introduced into the upper duct, while the diluted fuel is injected into the lower duct. The fuel stream consists of the fuel diluted with nitrogen. The two ducts are separated by a distance L. Autoignition experiments were carried out at L = 14 mm, while L = 12 mm was used for extinction experiments. The fuel mass fraction, temperature, density of the fuel stream, and the component of the fuel flow velocity normal to the stagnation plane at the exit of the fuel outlet are $Y_{f,1}$, T_1, ρ_1, and V_1, respectively. The oxygen mass fraction, oxidizer temperature, density and the oxidizer flow velocity normal to the stagnation plane at the exit of the oxidizer outlet are $Y_{O2,2}$, T_2, ρ_2, and V_2, accordingly. The diameters d, of the oxidizer and the fuel ducts are both 23 mm. All experiments were conducted assuming plug flow conditions, and also, by keeping the momenta of the counterflowing streams equal ($\rho V_i^2, i = 1,2$). The strain rate, a_2, Eq. (1), is defined as the gradient of the normal component of the flow velocity. This value changes from the exits of the fuel to oxidizer ducts respectively.[21] The assessment of the experimental strain rate in this study

was performed in accordance with the procedure outlined by Niemann et al.,[22] were also the explicit derivation of the characteristic strain rate is provided.

Autoignition experiments were conducted at $T_1 \approx 400$ K (±15 K) and $Y_{f,1} = 0.4$. At a certain strain rate a_2, the temperature of the oxidizer was slowly raised by controlling the voltage to the heating element, until autoignition occurred. The temperature of the air at the exit of the oxidizer duct just before autoignition occurred, T_2, was measured using a Pt-Pt 13% Rh-type thermocouple with a bead diameter of 0.015 mm. All oxidizer temperatures, $T_{2,i}$, were corrected to account for the heat lost due to radiation using Nusselts number, $Nu = 2$ and a constant emissivity, $e = 0.1$. The flow rates of the two counterflowing streams were continuously adjusted based on their temperature to ensure a balanced momentum.

Extinction experiments were also carried out at $T_1 \approx 400$ K (±10 K) and $T_2 = 298$ K. At a given fuel mass fraction $Y_{f,1}$, a stable flame is formed. The velocities of the two flowing streams V_1 and V_2 are gradually increased by increasing the flow rates whilst maintaining a balanced momentum of the two counterflowing streams until the flame is extinguished. The corresponding strain rate at extinction, $a_{2,E}$, which is given by Eq. (1), is recorded.

The accuracy of the measurement of the oxidizer temperature was determined to be ±20 K. The experimental repeatability of the recorded temperature of air at auto-ignition was ±5 K. The accuracies of the strain rate and fuel mass fraction were 5% and 3% of the recorded values, respectively. The experimental repeatability of the reported strain rate at extinction was 3% of the recorded value.

$$a_2 = \frac{2|V2|}{L}\left(1 + \frac{|V1|\sqrt{\rho_1}}{|V2|\sqrt{\rho_2}}\right) \quad (1)$$

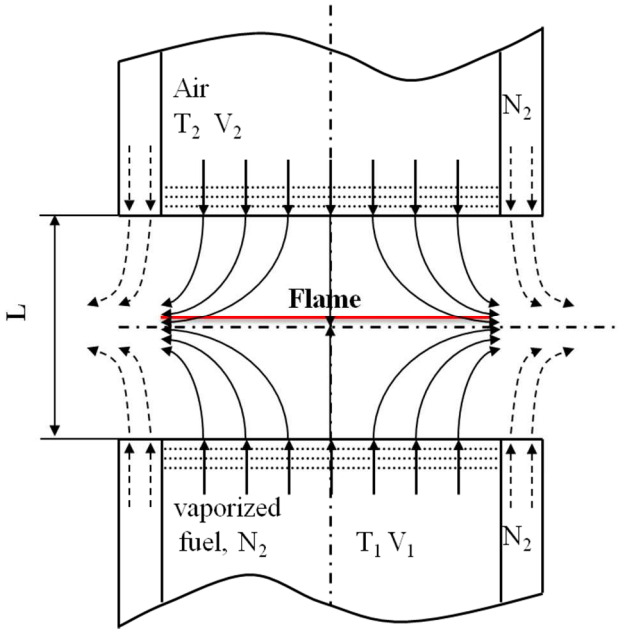

Figure 1. Schematic diagram of the counterflow system

2.2. Numerical procedure

The numerical simulations were carried out with CHEMKIN PRO.[23] For ignition simulations, a detailed high-temperature alcohol combustion mechanism by Sarathy et al.[1] was used. The model comprises of 354 species and over 2400 chemical reactions and includes a complete C1-C5 alcohols sub-mechanism. For extinction simulations, a skeletal mechanism derived from the abovementioned mechanism was utilized. The skeletal model consists of 205 species plus 1539 chemical reactions. It was generated manually by adding high-temperature sub-mechanisms for C1-C5 alcohols to the skeletal mechanism from Sarathy et al.'s iso-pentanol study.[24]

Flame ignition simulations were conducted using the OPPDIF solver available in CHEMKIN PRO.[23] First, a temperature profile was established with cold mixtures at fuel and oxidizer inlets, and then the temperature of the oxidizer inlet was gradually raised until ignition occurred. The composition of the reactants and the temperature of the fuel stream, T_1, were kept constant while carrying out this process. The calculations were carried out with thermal diffusion, mixture-

averaged transport and convergence parameters of GRAD = 0.1 and CURVATURE = 0.1. GRAD and CURVATURE are adaptive grid control parameters that control the extent to which the solution gradient and curvature is resolved.

For extinction simulations, the extinction solver in CHEMKIN-PRO was employed. The solver uses an arc length continuation method to generate the S-curve. At first, a stable flame was established using the OPPDIF code at conditions near extinction, then this solution was restarted in the extinction solver. A 2-point extinction method with 1000 steps was used. Large convergence factors (GRAD 0.1 and CURVATURE 0.5) were used to control the maximum gradients and curvatures allowed between grid points. Thermal diffusion and a mixture-average transport were employed to determine the species diffusion coefficients and fluxes.

3. Results and Discussion

3.1 Autoignition results

Counterflow diffusion flame autoignition experiments were conducted using the procedure described in the preceding section. Figure 2 presents the temperature of the air at autoignition as a function of strain rate. The experimental results show that a higher oxidizer temperature is required to achieve autoignition when the strain rate increases. The temperature required for fuel autoignition increased in the following order: *iso*-propanol > *iso*-butanol > *1*-butanol ≈ *n*-propanol. This trend clearly demonstrates the effect of chain substitution in decreasing the reactivity of the branched alcohols. Similar observations were also made on normal and branched hydrocarbons by.[17,18,25,26] Those studies noted that increase in methyl substitutions leads to the formation of less reactive intermediates, some of which are resonantly stable, thereby decreasing the overall reactivity. Overall, the model was able to predict the trends observed in the experiment except for *n*-propanol. The simulated results on Fig. 2 under predict the ignition

temperatures for *n*-propanol, and, contrary to the experiments, that *n*-propanol ignites faster than *1*-butanol.

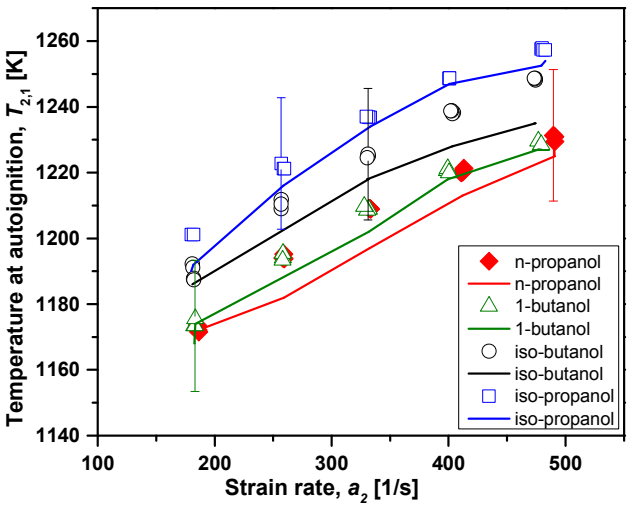

Figure 2. Air temperature at autoignition, $T_{2,1}$ as a function of strain rate, a_2. Symbols are experimental data, and lines represent modelling predictions. Error bars represents the uncertainties in ignition temperature measurements.

3.2 Extinction results

The procedures described in previous section were used for counterflow extinction experiments. Figure 3 shows the mass fraction of fuel as a function of strain rate for both experiments and simulations. The experimental result shows that extinction limits for these tested alcohols are in the following order: *n*-propanol ≈ *1*-butanol > *iso*-butanol > *iso*-propanol. In other words, *n*-propanol and *1*-butanol flames are the most difficult to extinguish while *iso*-propanol flame is the easiest to extinguish, which demonstrates the effect of substitution on the lower extinction limits in the iso-alcohols.

Experimental results on Fig. 2 and Fig. 3 show that *1*-butanol and *n*-propanol have similar autoignition temperatures and extinction limits. Similar trends were previously observed by Veloo et al.,[9] Beeckmann et al.[7] and Sarathy et al.,[1] wherein all normal C3-C5 alcohols were shown to have similar laminar flame speeds. The agreement between the experimental data and the model prediction is acceptable, except for *n*-propanol. The simulation over predicted the reactivity of *n*-propanol and suggests that *n*-propanol is slightly more reactive than *1*-butanol. The reason for this behavior by the model is investigated in next section.

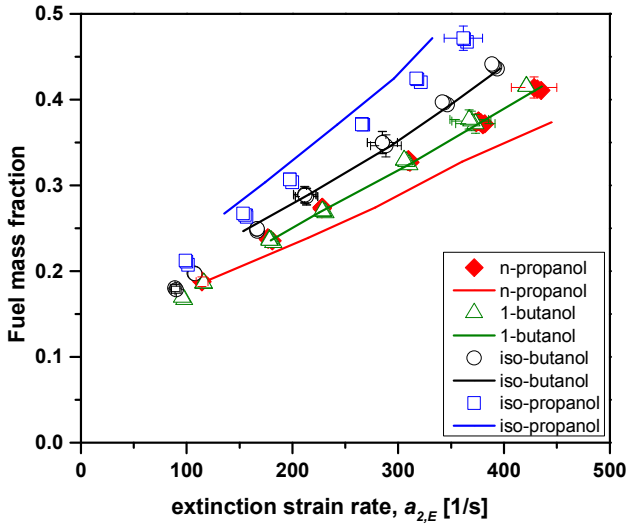

Figure 3. The mass fraction of fuel as a function of strain rate at extinction, $a_{2,E}$ in the Counterflow diffusion flame. Symbols represent experimental data, and lines are modelling predictions. Error bars represents the expected uncertainty in fuels mass fraction and extinction strain rates.

A plot of fuel mole fraction (instead of mass fraction) versus extinction strain rate would show the following order based on an increase in the extinction limits: *1*-butanol > *n*-propanol > *iso*-butanol > *iso*-propanol. This reversed order in reactivity when comparing extinction limits on

molar basis was also observed by Won et al.,[27] because on a mole fraction basis, this order is based on the combined effects of mass diffusion, fuel potential energy and kinetics.[27] To understand the kinetic contribution towards diffusion flame extinction, Won et al. introduced the transport weighted enthalpy (TWE) concept. It is defined as a product of fuel concentration [fuel], heat of combustion (ΔH_c), and inverse of the square root of the ratio of fuel molecular weight to nitrogen molecular weight $(MW_{fuel}/MW_{N2})^{-1/2}$. The use of this expression enables the normalization of the molecular transport and thermal contribution towards diffusion flame extinction. Therefore, the difference in reactivity of fuels can be determined by plotting extinction strain rates against the transport weighted enthalpy.[27,28] Figure 4 is a graph of extinction strain rate versus TWE. Thus, plotting extinction strain rate versus TWE reverses this order to *n*-propanol > *1*-butanol > *iso*-butanol > *iso*-propanol, thereby rationalizing the use of extinction strain rate to explain reactivity of fuels based on their ability to form radicals.

In addition to TWE, Won et al. introduced a term, fuel radical index (Ri), to quantitatively describe the kinetic role of fuel chemistry, based on the ability of a particular fuel to produce H or OH radical concentrations in a flame relative to a normal alkane.[17,27] The TWE and Ri are based on the premise that the rates of heat release in the reaction zones are highly sensitive to diffusivities of fuel, OH and H radicals. Thus, flame quenching is less likely in fuels that produce more of these radicals. For this reason, simulations were carried out at fixed TWE ~ (2.46), strain rate ~ (250 s^{-1}), and initial fuel temperature, T_1 = 125 C, to calculate Ri_H and Ri_{OH}. Propanol was used as a base fuel and the result is shown in Table (1). The choice of *n*-propanol as a base fuel is because previous findings[1,9,29] have shown that normal alcohols have comparable laminar flame speeds as normal alkanes. The order in terms of ability of these fuels to produce OH and H radicals is as follows: *n*-propanol > *1*-butanol > *iso*-butanol > *iso*-propanol, which clearly

explains the reason for the observed differences in extinction limits of these fuels by the model. Figure 5 shows that the extinction strain rate of all fuels would be almost the same when plotted as a function of TWE*Ri. Note, correlations from present study agree with the data by Won et al. This agreement illustrates the suitability of the radical index concept for various fuels.

Table 1. Summary of radical indexes Ri_H and Ri_{OH} of the candidate fuels

Fuel	Ri_{OH}	Ri_H
1-butanol	0.94	0.93
n-propanol	1	1
iso-butanol	0.89	0.85
iso-propanol	0.68	0.58

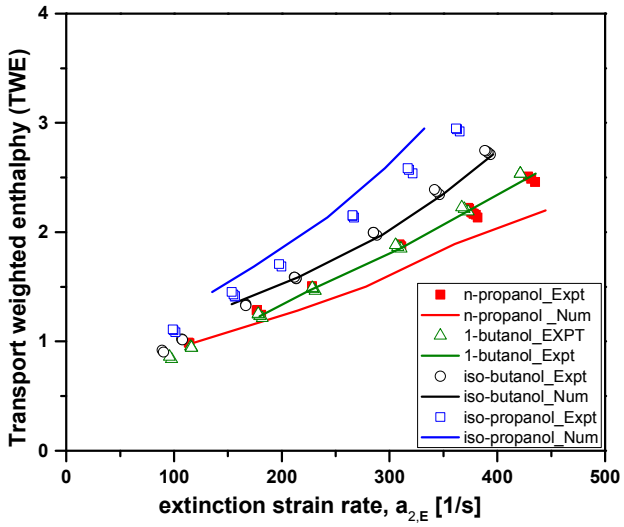

Figure 4. Extinction limits at different TWE. TWE = $([fuel]*\Delta Hc*MW_{fuel}/MW_{N2})^{-1/2}$ cal/cm^3)

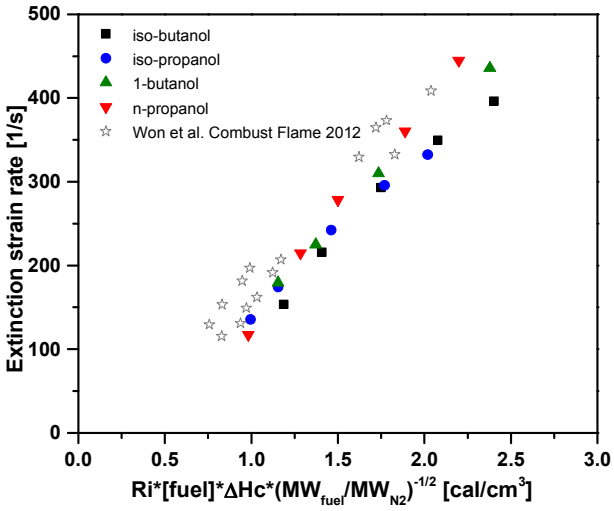

Figure 5. General correlations of extinction strain rates as a function of the product of transport weighted enthalpy and radical index. Open symbols are data from Won et al.[27], and closed symbols represent current study.

To further understand why *n*-propanol produce more Ri_H and Ri_{OH} according to the model, and consequently higher reactivity as compared to *1*-butanol, computational analyses of the concentration profiles were carried out at a fixed TWE = 2.0 and initial fuel temperature T_f = 398 K. Additionally, integrated flux analyses were performed on these fuels, to understand the controlling kinetic mechanisms of their oxidation. Figure 6a and Fig. 6c reveals that there is a high amount of propene and propargyl intermediates in *1*-butanol as compared to *n*-propanol. On the contrary, the amount of propanal and formaldehyde produced by *n*-propanol is higher (21 and 1.5 times respectively) than the amount produced by *1*-butanol. Previous studies have shown that the presence of higher concentration of propene in the reaction pool decreases the reactivity.[5] Likewise, the comparison of the flux analyses in Fig. 7a and Fig. 7c proved that while several pathways produce propene and propargyl radical in *1*-butanol, only few percent of the pathways yield propene from *n*-propanol flames. The majority of intermediates from *n*-propanol oxidation

favor the formation of formaldehyde and propanal, which decompose into formyl radicals and eventually lead to the production of more active radicals. Almost 78% of propene in *1*-butanol flames are produced through the reaction of C_4H_8OH-3 ⇔ C_3H_6 + CH_2OH, which subsequently consumes active radicals to form a resonantly stable allyl species C_3H_5-a. The preferred pathway for the reaction of propargyl radical is the consumption of atomic hydrogen to form C_3H_4-p. Subsequently, the high concentration of propene and propargyl in the *1*-butanol flame consumes the fewer OH and H produced by *1*-butanol, hence lowering its reactivity as compared to *n*-propanol.

Similar analysis was made to understand the effects of substitution on the observed reactivities of the tested alcohols. Figure 6 shows that the OH/CH_3-substituted alcohols produce almost twice the amount of propene and propargyl as compared to *n*-alcohols; consequently they produce a less reactive pool of intermediates. A comparison of *n*-propanol and *iso*-propanol fluxes in Fig. 7a and Fig. 7b respectively reveals that a greater percentage of the latter results in the formation of propene and propargyl intermediates when compared to *n*-propanol. In addition, while a large percentage of less reactive acetone is formed in *iso*-propanol flames, a majority of the intermediates produced in *n*-propanol would subsequently yield active radicals. As for C4-alcohols, a similar comparison can be made between the flux analyses in Fig. 7c and Fig. 7d. These comparisons show that *iso*-butanol produces a high percentage of *iso*-butene intermediates, whose succeeding reactions consume active radicals to form propene and allyl radical. Fewer such pathways are observed in *1*-butanol as compared to *iso*-butanol flames. Hence, the formation of a higher amount of less reactive intermediate in *iso*-propanol and *iso*-butanol flames suggests their role in decreasing the overall reactivities of these fuels.

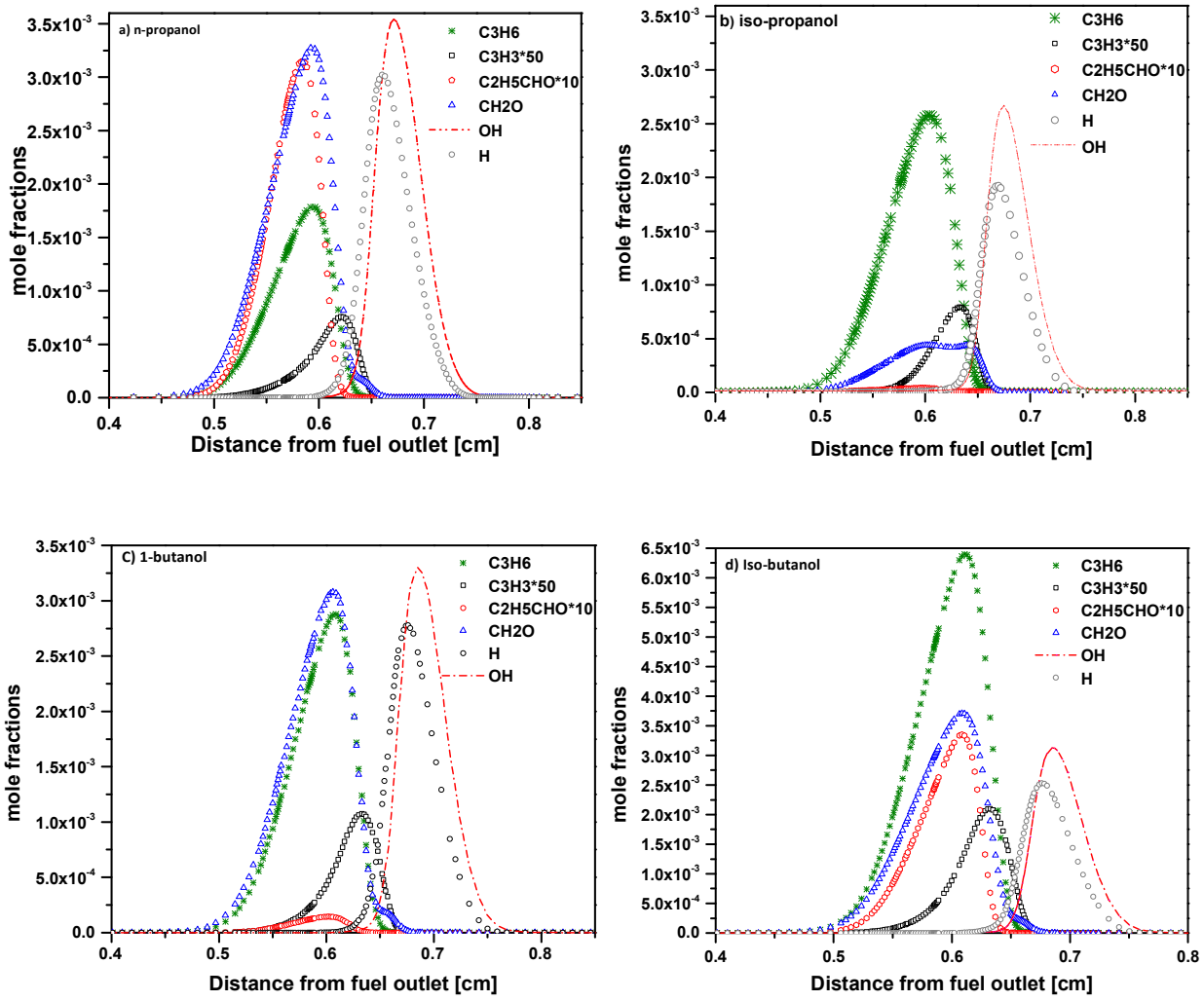

Figure 6. Comparison of concentration profiles from the oxidation of: (a) *n*-propanol (b) *iso*-propanol (c) *1*-butanol (d) *iso*-butanol

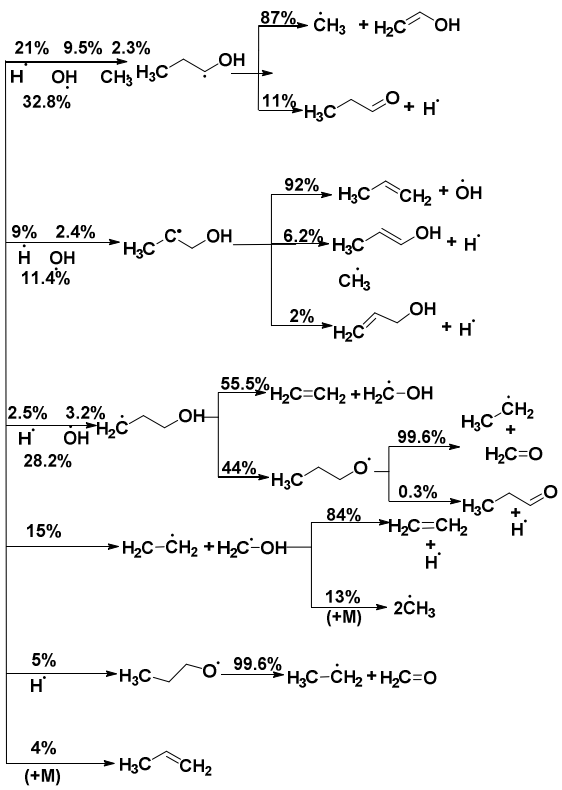

(a)

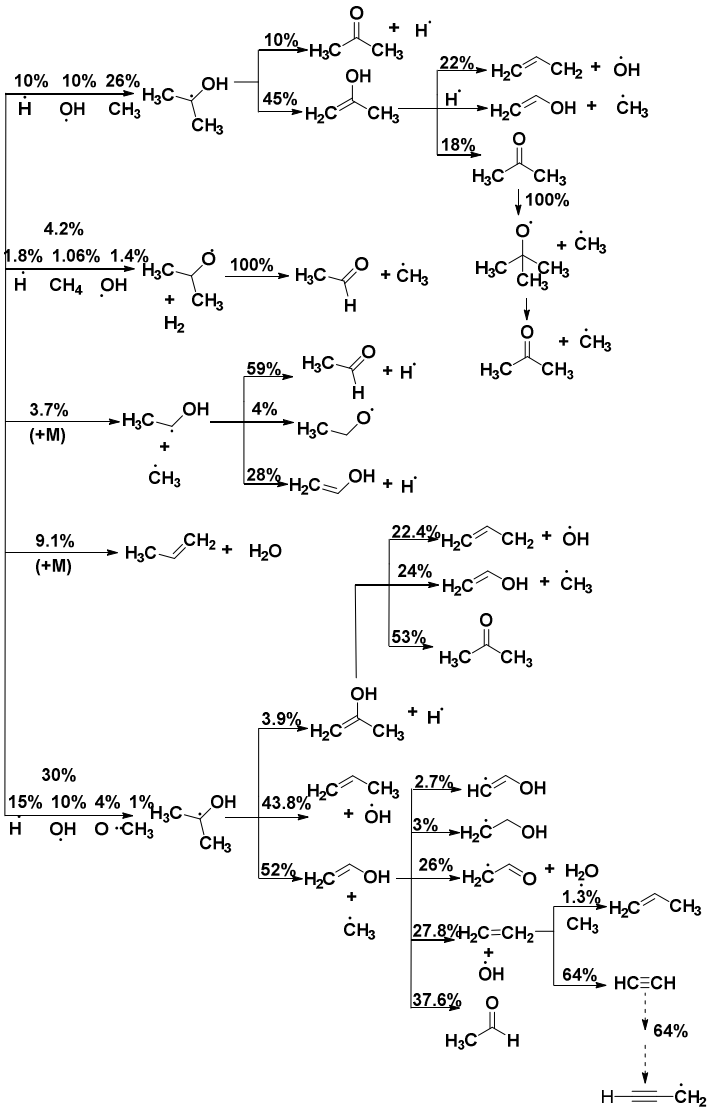

(b)

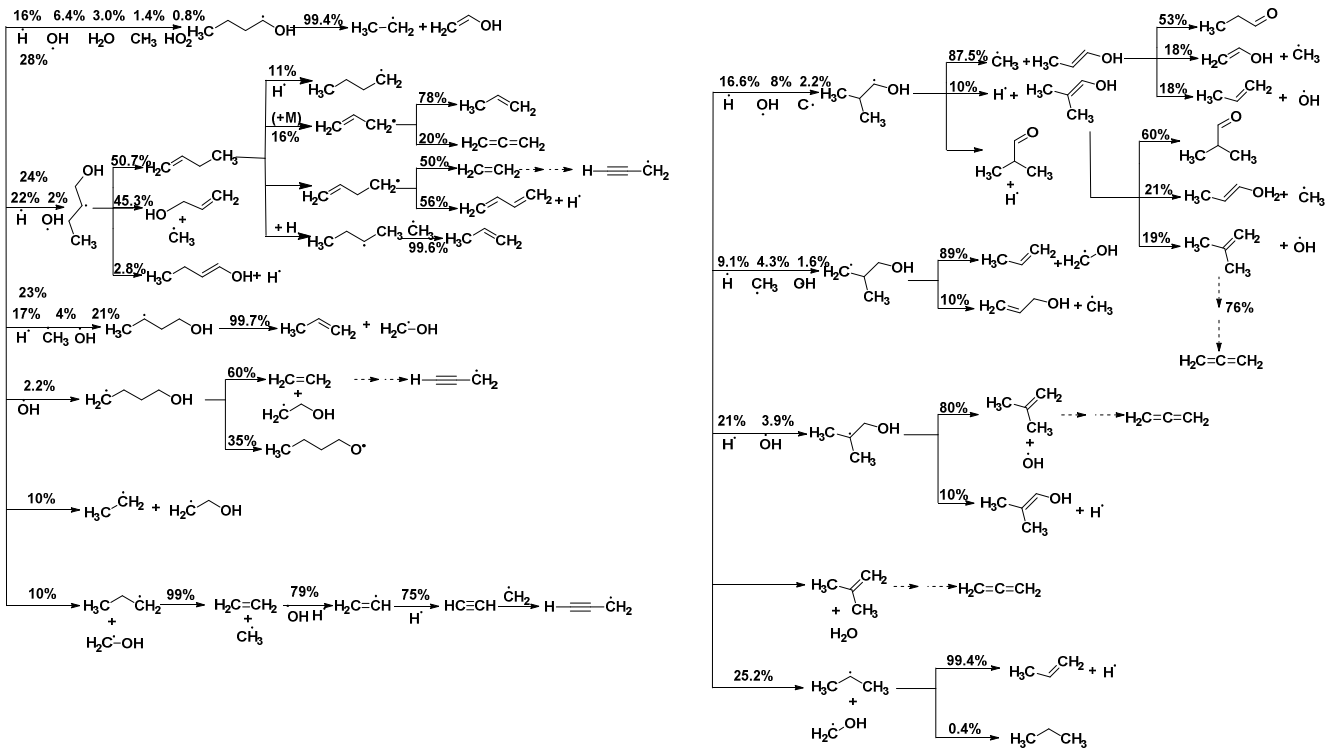

(c) (d)

Figure 7. Flux analysis showing the major pathways for all the tested fuels and intermediates consumption at fixed TWE; numbers indicate consumption percentage (a) *n*-propanol (b) *iso*-propanol (c) *1*-butanol (d) *iso*-butanol

4. Conclusions

In the present study, experiments were conducted using the counterflow flame apparatus. Experimental data was obtained on autoignition temperatures and extinction strain rates of four alcohol fuels. Numerical simulations were performed and the predicted results were compared to the experiments. Overall, the quantitative agreement between the model and the experiments is acceptable. The experimental results showed that ignition temperatures of *1*-butanol are comparable to that of *n*-propanol, while the simulation over predicted the reactivity for *n*-propanol. Furthermore, experiments indicated that *n*-propanol and *1*-butanol flames have similar

extinction limits whereas simulated result suggests that *n*-propanol flame is more resistant to extinction. The inability of the model to accurately predict the trend in reactivity between *1*-butanol and *n*-propanol is further investigated through numerical simulations. The result revealed that *1*-butanol produces higher concentrations of propene and propargyl radicals, which slows down its overall reactivity. On the other hand, *n*-propanol produces more formaldehyde and propanal whose subsequent reactions produces more active radicals, thereby enhancing further reactions. Radical index analysis also showed that *n*-propanol produces more OH and H radicals, thereby increasing the ability to sustain a diffusion flame compared to *1*-butanol.

Similarly, the amount of propene and propargyl produced by the substituted alcohols is significantly higher than the amount produced by normal alcohols, thereby consuming the active radicals produced to form relatively stable intermediates, and probably rationalizing lower reactivity in the former.

AUTHOR INFORMATION

Corresponding Author

*Mani S. Sarathy, King Abdullah University of Science and Technology (KAUST), Clean Combustion Research Center (CCRC), Thuwal 23955-6900, Saudi Arabia. E-mail: Mani.Sarathy@kaust.edu.sa

*Adamu Alfazazi, King Abdullah University of Science and Technology (KAUST), Clean Combustion Research Center (CCRC), Thuwal 23955-6900, Saudi Arabia. E-mail: Adamu.Fazazi@kaust.edu.sa

Notes:

The authors declare no competing financial interest.

ACKNOWLEDGMENT

This work was performed by the Clean Combustion Research Center with funding from King Abdullah University of Science and Technology (KAUST) and Saudi Aramco under the FUELCOM program. Research reported in this publication was also supported by competitive research funding from KAUST. The research at the University of California at San Diego was supported by UC Discovery/West Biofuels, LLC Grant # GCP06-10228. We thank Professor Kalyanasundaram Seshadri, Samah Y. Mohammed and Nour Atef for their contribution.

ABBREVIATIONS

TWE, Transport weighted enthalpy; Ri, radical index; $Y_{f,1}$, fuel mass fraction; X_f, fuel mole fraction, T_1, fuel temperature; ρ_1, density of the fuel stream, V_1 fuel flow velocity; $Y_{O2,2}$, oxygen mass fraction, T_2, oxidizer temperature; ρ_2 oxidizer density; V_2, oxidizer velocity.

REFERENCES

(1) Sarathy, S. M.; Oßwald, P.; Hansen, N.; Kohse-Höinghaus, K. *Prog. Energy Combust. Sci.* **2014**, *44*, 40–102.

(2) Frassoldati, A.; Cuoci, A.; Faravelli, T.; Niemann, U.; Ranzi, E.; Seiser, R.; Seshadri, K. *Combust. Flame* **2010**, *157* (1), 2–16.

(3) Agarwal, A. K. *Prog. Energy Combust. Sci.* **2007**, *33* (3), 233–271.

(4) Moss, J. T.; Berkowitz, A. M.; Oehlschlaeger, M. A.; Biet, J.; Warth, V.; Glaude, P.-A.; Battin-Leclerc, F. *J. Phys. Chem. A* **2008**, *112* (43), 10843–10855.

(5) Veloo, P. S.; Egolfopoulos, F. N. *Proc. Combust. Inst.* **2011**, *33* (1), 987–993.

(6) NOORANI, K. E.; AKIH-KUMGEH, B.; BERGTHORSON, J. M. *Energy & fuels 24* (NOV-DEC), 5834–5843.

(7) Beeckmann, J.; Cai, L.; Pitsch, H. *Fuel* **2014**, *117*, 340–350.

(8) Veloo, P. S.; Wang, Y. L.; Egolfopoulos, F. N.; Westbrook, C. K. *Combust. Flame* **2010**, *157* (10), 1989–2004.

(9) Veloo, P. S.; Egolfopoulos, F. N. *Combust. Flame* **2011**, *158* (3), 501–510.

(10) Johnson, M. V.; Goldsborough, S. S.; Serinyel, Z.; O'Toole, P.; Larkin, E.; O'Malley, G.; Curran, H. J. *Energy and Fuels* **2009**, *23* (12), 5886–5898.

(11) Wang, H.; You, X.; Joshi, V. A.; Davis, G. S.; Laskin, A.; Fokion, E.; Law, C. K. .

(12) Brady, K. B.; Hui, X.; Sung, C.-J.; Niemeyer, K. E. *Combust. Flame* **2015**, *162* (10), in press doi:10.1016/j.combustflame.2–15.09.026.

(13) Hashimoto, J.; Tanoue, K.; Taide, N.; Nouno, Y. *Proc. Combust. Inst.* **2015**, *35* (1), 973–980.

(14) Mitsingas, C. M.; Kyritsis, D. C. *J. Energy Eng.* **2014**, *140* (3), A4014006.

(15) Sarathy, S. M.; Vranckx, S.; Yasunaga, K.; Mehl, M.; Oßwald, P.; Metcalfe, W. K.; Westbrook, C. K.; Pitz, W. J.; Kohse-Höinghaus, K.; Fernandes, R. X.; Curran, H. J. *Combust. Flame* **2012**, *159* (6), 2028–2055.

(16) Merchant, S. S.; Zanoelo, E. F.; Speth, R. L.; Harper, M. R.; Van Geem, K. M.; Green, W.

H. *Combust. Flame* **2013**, *160* (10), 1907–1929.

(17) Mani Sarathy, S.; Niemann, U.; Yeung, C.; Gehmlich, R.; Westbrook, C. K.; Plomer, M.; Luo, Z.; Mehl, M.; Pitz, W. J.; Seshadri, K.; Thomson, M. J.; Lu, T. *Proc. Combust. Inst.* **2013**, *34* (1), 1015–1023.

(18) Liu, N.; Ji, C.; Egolfopoulos, F. N. *Combust. Flame* **2012**, *159* (2), 465–475.

(19) Seiser, R.; Pitsch, H.; Seshadri, K.; Pitz, W. J.; Curran, H. J. *Proc. Combust. Inst.* **2000**, *28* (2), 2029–2037.

(20) Humer, S.; Seiser, R.; Seshadri, K. *Proc. Combust. Inst.* **2002**, *29* (2), 1597–1604.

(21) Seshadri, K.; Williams, F. A. *Int. J. Heat Mass Transf.* **1978**, *21* (2), 251–253.

(22) Niemann, U.; Seshadri, K.; Williams, F. a. *Combust. Flame* **2014**, *162* (4), 1540–1549.

(23) CHEMKIN-PRO Release 15113. San Diego 2015.

(24) Mani Sarathy, S.; Park, S.; Weber, B. W.; Wang, W.; Veloo, P. S.; Davis, A. C.; Togbe, C.; Westbrook, C. K.; Park, O.; Dayma, G.; Luo, Z.; Oehlschlaeger, M. A.; Egolfopoulos, F. N.; Lu, T.; Pitz, W. J.; Sung, C.-J.; Dagaut, P. *Combust. Flame* **2013**, *160* (12), 2712–2728.

(25) Davis, S. G.; Law, C. K. *Combust. Sci. Technol.* **1998**, *140* (1-6), 427–449.

(26) Selim, H.; Mohamed, S. Y.; Lucassen, A.; Hansen, N.; Sarathy, S. M. *Energy and Fuels* **2015**, *29* (4), 2696–2708.

(27) Won, S. H.; Dooley, S.; Dryer, F. L.; Ju, Y. *Combust. Flame* **2012**, *159* (2), 541–551.

(28) Lefkowitz, J. K.; Heyne, J. S.; Won, S. H.; Dooley, S.; Kim, H. H.; Haas, F. M.; Jahangirian, S.; Dryer, F. L.; Ju, Y. *Combust. Flame* **2012**, *159* (3), 968–978.

(29) Ranzi, E.; Frassoldati, A.; Grana, R.; Cuoci, A.; Faravelli, T.; Kelley, A. P.; Law, C. K. *Prog. Energy Combust. Sci.* **2012**, *38* (4), 468–501.